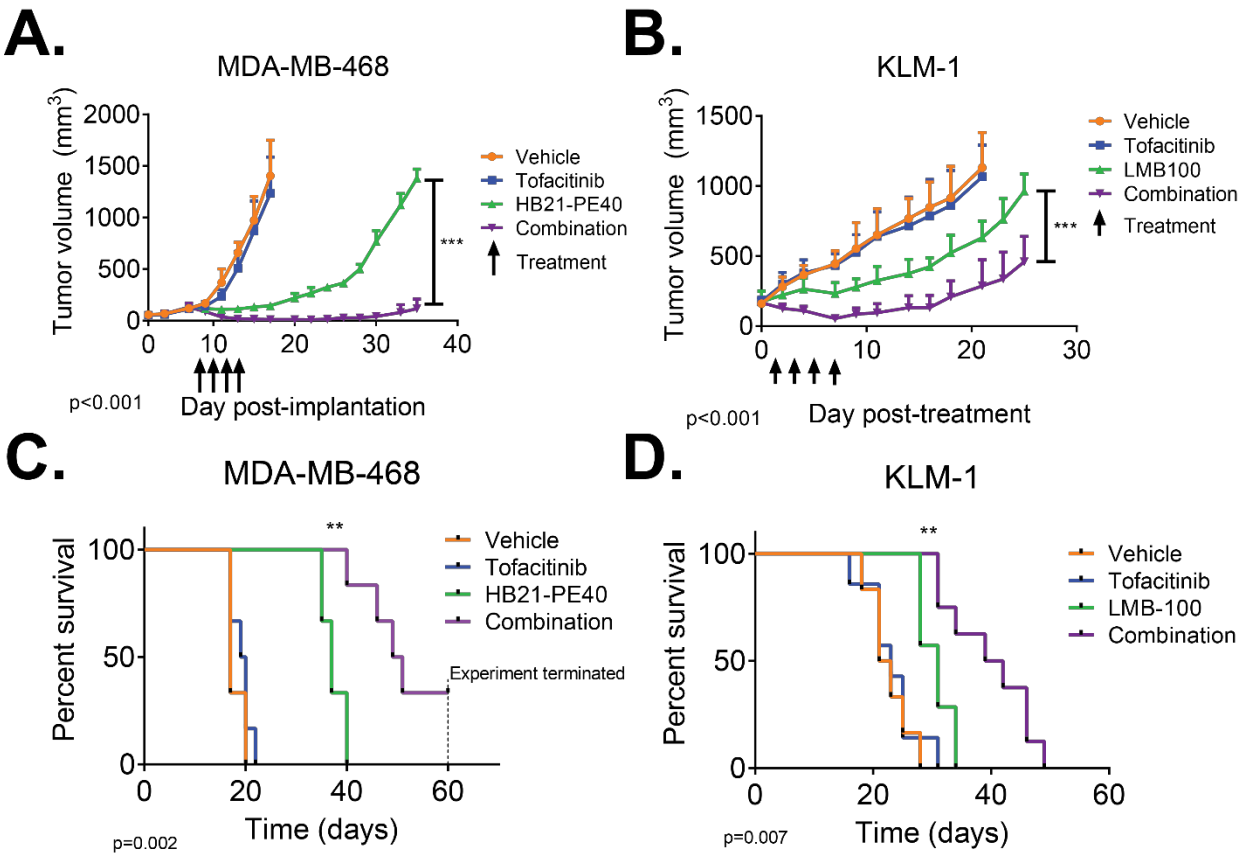

Supplemental Figure 1. Tofacitinib shows enhancement of immunotoxin activity in vivo. A. Mice bearing MDA-MB-468 TNBC tumors were treated with vehicle, tofacitinib alone, immunotoxin alone, or the combination of both treatments (4 x qod; arrows). Tumor volumes were measured at least twice weekly. Tumor volumes for each treatment group were compared by two-tailed t-test at each time point. *** $p<0.001$. B. Mice bearing KLM-1 PDAC tumors were treated with vehicle, tofacitinib alone, immunotoxin alone, or the combination of both treatments (4 x qod; arrows). Tumor volume was measured at least twice weekly. Tumor volumes for each treatment group were compared by two-tailed t-test at each time point. *** $p<0.001$. C. Kaplan-Meyer plot displaying time-to-death of each treatment group for mice implanted with MDA-MB-468 tumors. Mice were euthanized once tumor volume reached 1000mm3. Log-rank test was performed to calculate significance. ** $p<0.01$ compared to immunotoxin treated. D. Kaplan-Meyer plot displaying time-to-death of each treatment group for mice implanted with KLM-1 tumors. Mice were euthanized once tumor volume reached 1200mm3. Log-rank test was performed to calculate significance. ** $p>0.01$ compared to immunotoxin –treated.

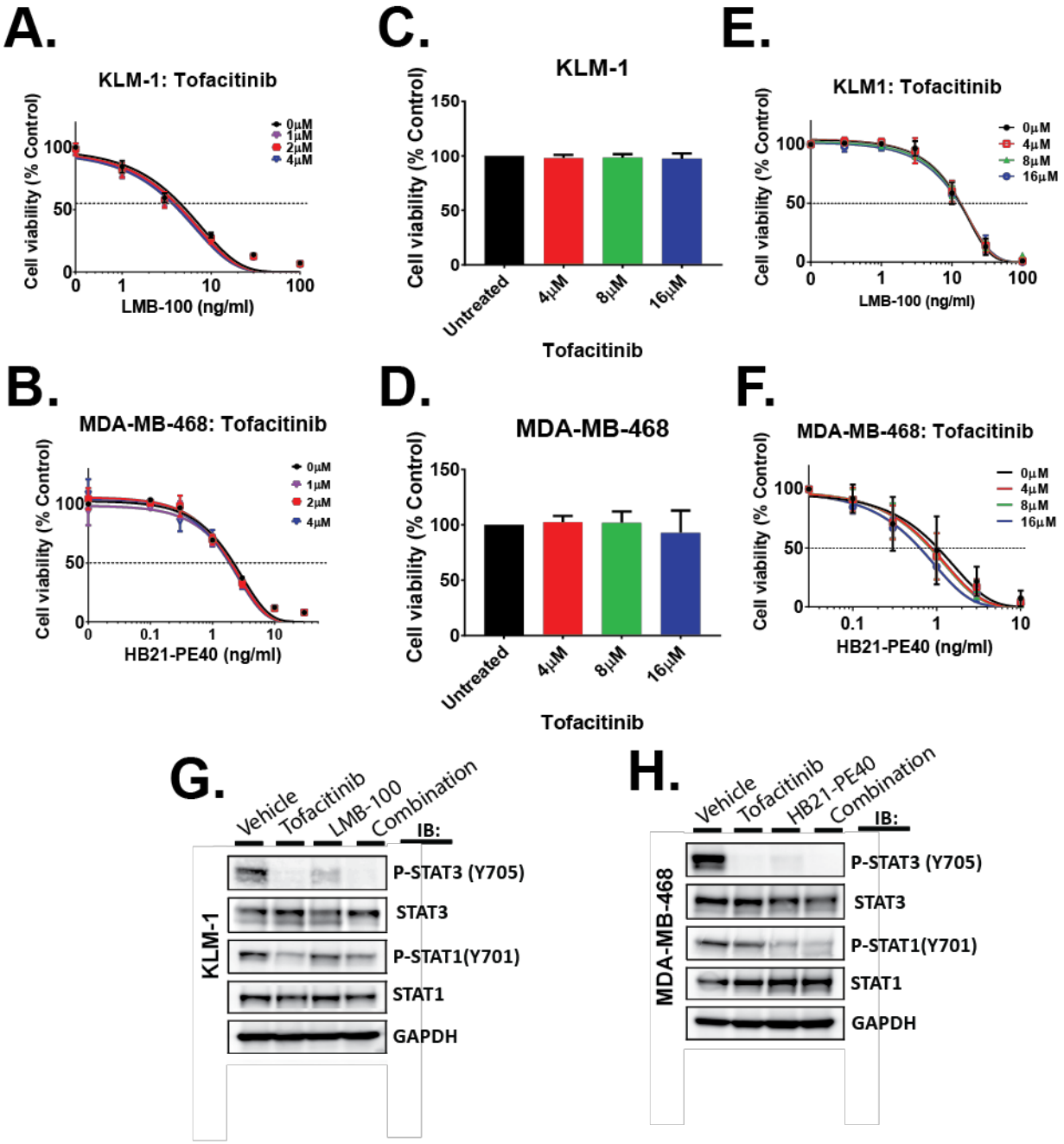

Supplemental Figure 2. Tofacitinib does not enhance immunotoxin activity *in vitro.*

A. KLM-1 or B. MDA-MB-468 cells were incubated with the indicated concentration of immunotoxin and tofactinib. Immunotoxins at the indicated concentrations were incubated alone or in the presence of increasing concentrations of tofacitinib for 72 hr. Cell viability was measured

using CellTiterGlo and normalized to non-immunotoxin treated controls. C. MDA-MB-468 or D. KLM-1 cells were treated with concentrations of tofacitinib up to 16μM. Cell viability was measured after 72 hours with no significant changes observed. E. MDA-MB-468 or F. KLM-1 cells were incubated with the indicated concentrations of tofactinib and immunotoxin. Cell viability was measured after 72 hours, with tofactinib showing little enhancement of immunotoxin activity *in vitro*. G. KLM-1 or H. MDA-MB-468 cells were treated with vehicle (DMSO), 4μM tofacitinib, 10ng/ml HB21-PE40 or 100ng/ml LMB-100, or the combination of both. After 24 hours, the cells were lysed and immunoblotted for selected activated or total STAT proteins. Protein loading was normalized to GAPDH.

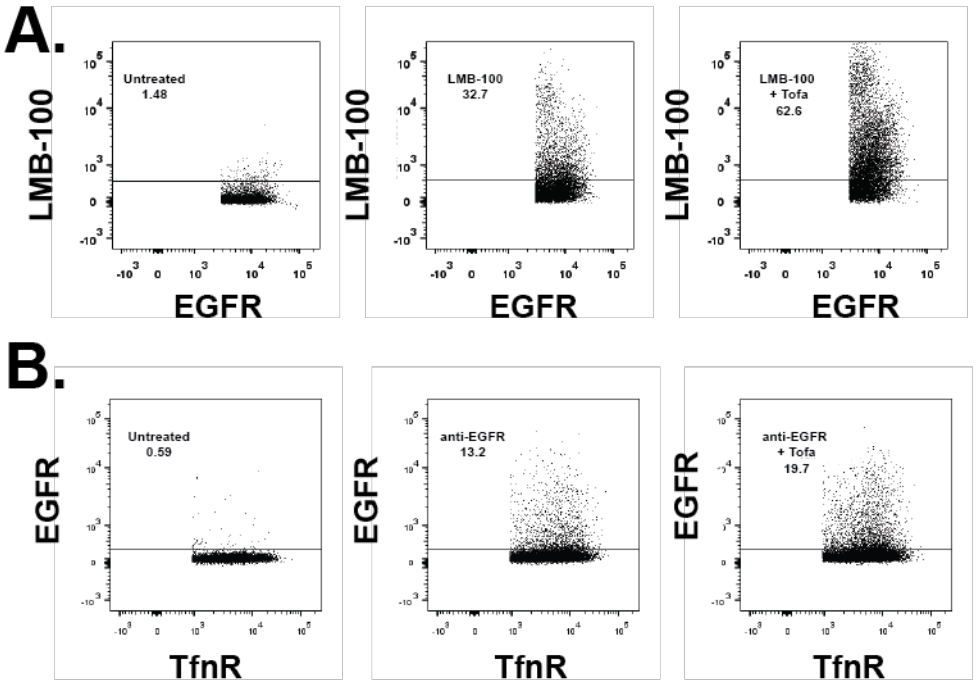

Supplemental Figure 3. Tofacitinib enhances the delivery of antibody-based therapeutics to malignant cells.

A. Mice bearing KLM-1 tumors were treated with fluorescently labeled LMB-100 immunotoxin. After 3 hours, tumors were harvested and dissociated into single cell suspensions, with tumor cells identified by anti-human EGFR. Tumor cells were then scored by flow cytometry for cell-associated immunotoxin. Representative plots are provided showing the uptake of labeled LMB-100 into KLM-1 tumor cells with and without tofacitinib. B. Mice bearing KLM-1 xenografts were injected with anti-EGFR—BV421 for 3 hours with or without tofacitinib. Human tumor cells were identified by incubation with anti-Transferrin receptor-APC. Representative plots showing KLM-1 tumor uptake EGFR-BV421 with and without tofacitinib are shown.

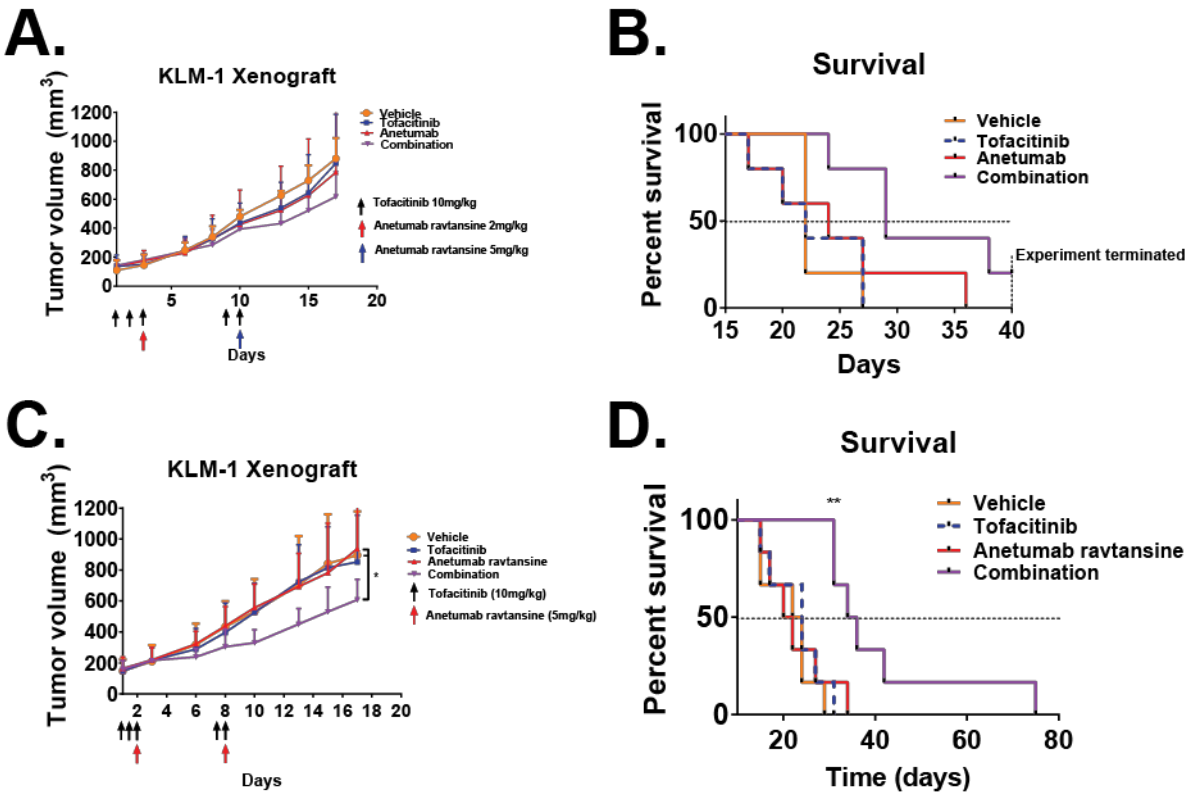

Supplemental Figure 4. Tofacitinib enhances ADC anti-tumor activity with low doses of anetumab ravtansine.

A. Mice bearing KLM-1 tumors were treated with vehicle, tofacitinib (black arrows), anetumab ravtansine (2.5mg/kg; red arrow; 5mg/kg; blue arrow) alone or in combination with tofacitinib. B. Kaplan-Meyer plot displaying time-to-death of each treatment group. Mice were euthanized once tumor volume reached 1200mm3 or became necrotic. Log-rank test was performed to calculate significance. ** $p<0.01$ compared to immunotoxin treated. C. Mice bearing KLM-1 tumors were treated with vehicle, tofacitinib alone, anetumab ravtansine (5mg/kg; red arrows) alone or the combination of both treatments. Tumor growth was compared by 2-way ANOVA. * $p<0.05$ D. Kaplan-Meyer plot displaying time-to-death of each treatment group. Log-rank test was performed to calculate significance. ** $p<0.01$ compared to immunotoxin treated.

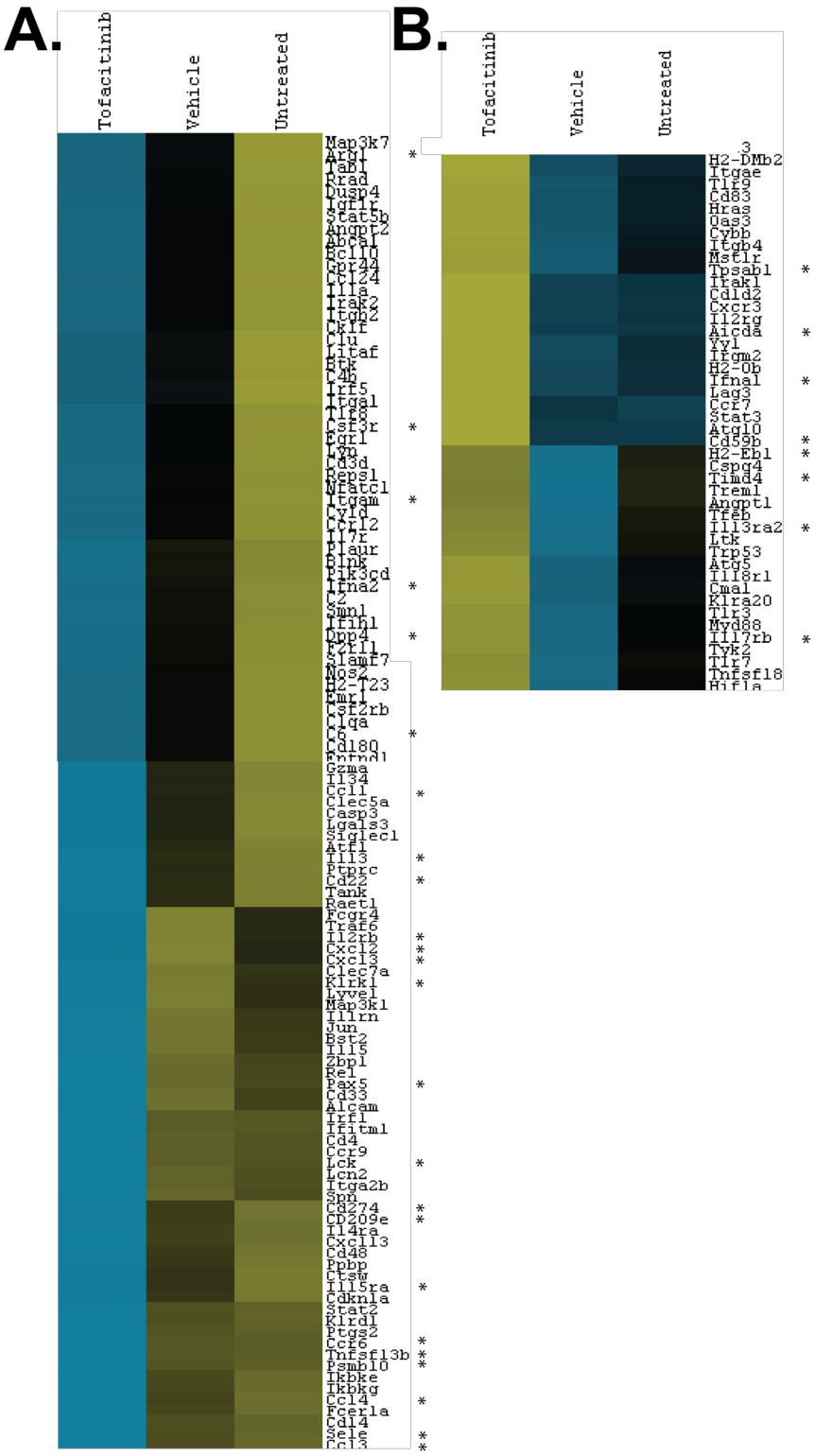

Supplementary Figure 5. Alterations in immune-related transcripts following tofacitinib treatment of mice with KLM-1 xenografts.

A, B. Nanostring heatmap analysis of differential murine mRNA transcript levels in untreated KLM-1 tumors, KLM-1 tumors treated with vehicle, or KLM-1 tumors treated with tofacitinib. Each treatment group consisted of n=3 animals. Yellow indicates upregulation of mRNA transcripts for the indicated gene and blue indicates mRNA transcript downregulation. Genes with >2-fold-decreases (A) or increases (B) between tofacitinib- and vehicle-treated mice are marked with *.

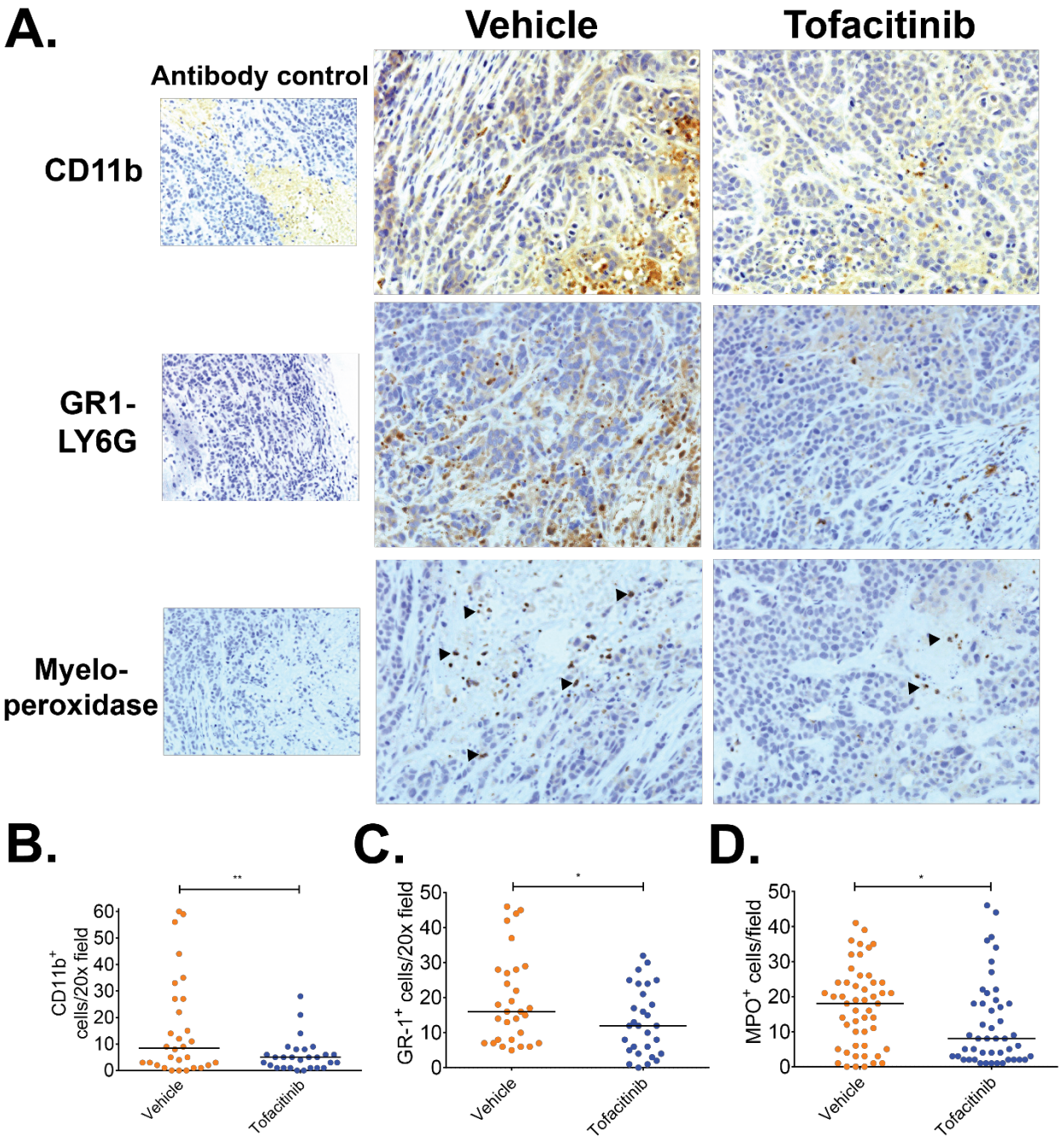

Supplemental Figure 6. Treatments with tofacitinib results in loss of MDA-MB-468 tumor-associated inflammatory cells.

A. Representative images of tumor-associated inflammatory cells in MDA-MB-468 xenografts after treatment with vehicle or tofacitinib. Total magnification is 320x. Xenograft sections were stained for CD11b (myeloid cells), GR1-LY6G (Granulocytes: neutrophils/myeloid suppressor cells), or myeloperoxidase (MPO; neutrophils; arrowheads). B. Quantification of tumor-associated myeloid cells for each treatment group. Cells staining positive for CD11b were counted from at least 20

randomly imaged fields, with counts from each field shown with the mean for each treatment. Significance was assessed by unpaired two-tailed t-test; ** $p<0.01$. C. Quantification of tumor-associated granulocytic cells for each treatment group. Cells staining positive for GR1-LY6G were counted from at least 20 randomly imaged fields, with counts from each field shown with the mean for each treatment. Significance was assessed by unpaired two-tailed t-test; * $p<0.05$. D. Quantification of tumor-associated neutrophils present for each treatment group. Cells staining positive for MPO were counted from at least 20 randomly selected fields, with counts from each field shown with the mean for each treatment. Significance was assessed by unpaired two-tailed t-test; * $p<0.05$.

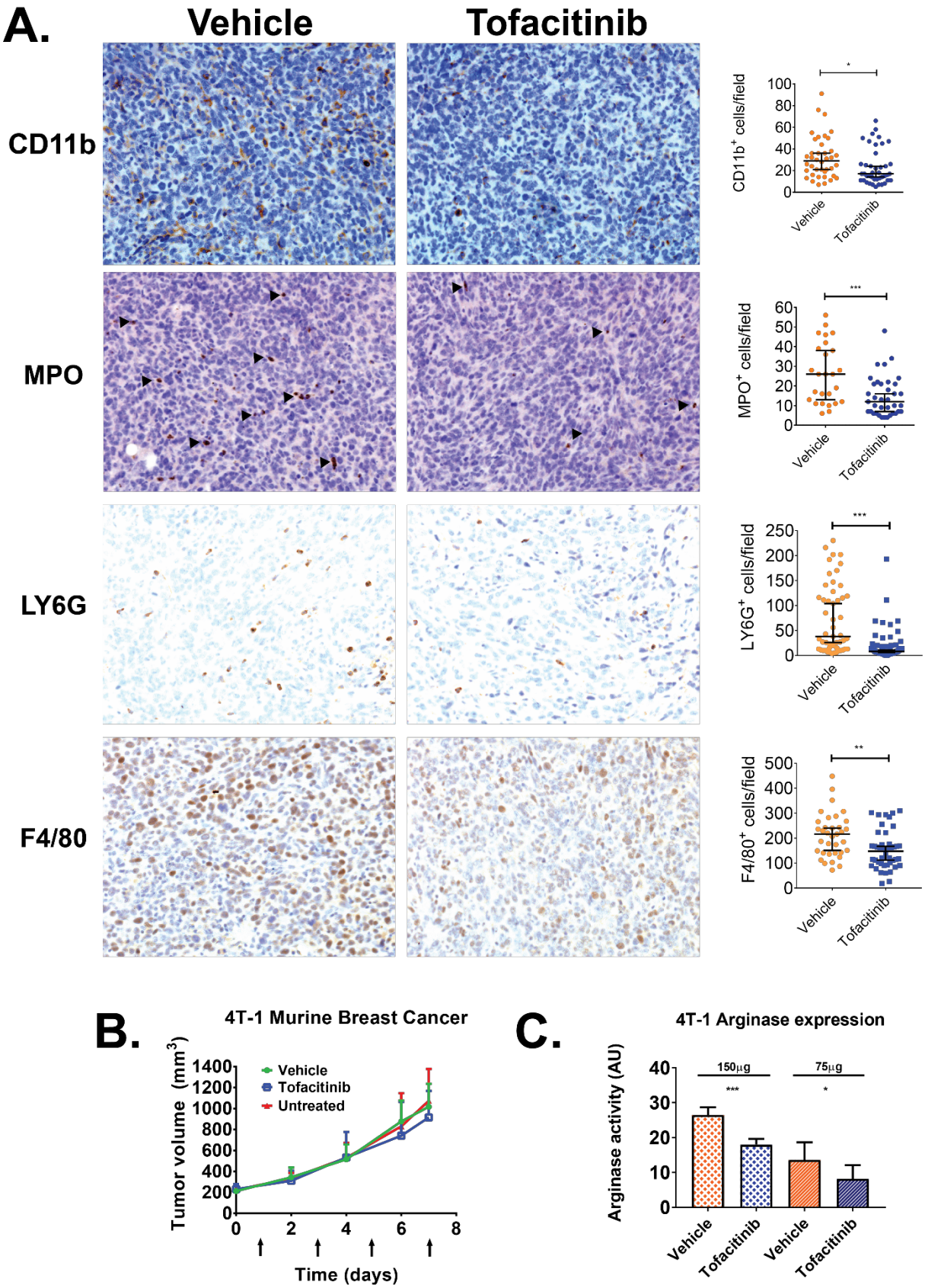
A.
Vehicle
Tofacitinib
CD11b
MPO
LY6G
F4/80
CD11b+ cells/field
MPO+ cells/field
LY6G+ cells/field
F4/80+ cells/field
Vehicle
Tofacitinib
B.
4T-1 Murine Breast Cancer
Tumor volume (mm3)
Vehicle
Tofacitinib
Untreated
Time (days)
C.
4T-1 Arginase expression
Arginase activity (AU)
150μg
75μg
Vehicle
Tofacitinib
Vehicle
Tofacitinib

Supplemental Figure 7. Response of 4T-1 tumors to treatments with tofacitinib

A. Representative images of myeloperoxidase (MPO), CD11b, F4/80, and LY6G staining of 4T-1 mouse breast cancer tumors from mice treated with tofacitinib or vehicle control. Total magnification is 320x. Quantification of tumor-associated cells for each marker for each treatment group is shown to the right. Cells staining positive for MPO, CD11b, F4/80, or LY6G were counted from at least 20 randomly selected fields, with counts from each field shown with the mean for each treatment. Significance was assessed by unpaired two-tailed t-test; * $p<0.05$, ** $p<0.01$, *** $p<0.001$. B. 4T-1 mouse breast cancer tumors were treated with one cycle (4x treatments QOD; arrows) of vehicle, tofacitinib, or left untreated. Tumor volumes were measured at least 3x weekly and compared by 2-way t-test at each time point. C. Arginase enzymatic activity was determined through colorimetric measurement of urea generated by arginase hydrolysis of L-arginine. One AU of arginase activity is identified as the amount of enzymatic activity required for production of 1μg urea in one hour. Results are averaged from 2 independent biological replicates utilizing either 75 or 150μg of homogenized tumor extract. Significance was assessed by 1-way ANOVA; * $p<0.05$, *** $p<0.001$.

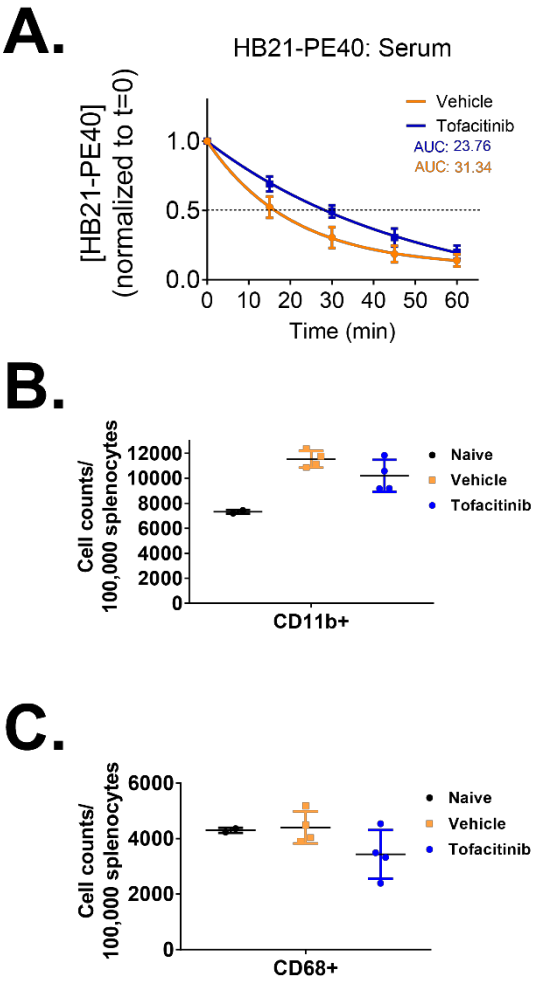

Supplementary Figure 8. Short-duration tofacitinib treatment reduces CD11b+ and CD68+ cells in the central compartment. A. Mice bearing MDA-MB-468 tumors were treated with vehicle or tofacitinib at T=-48 and -24 hours. At T=0, mice were injected intravenously with HB21-PE40 and blood was harvested at T=0, 15, 30, 45, and 60 minutes. Circulating HB21-PE40 and was detected by ELISA and normalized to a standard curve of purified HB21-PE40. The half-life and area under curve were calculated from best-fit regression analysis. Results are averaged from 2 biological replicates. B. Spleens harvested from naïve (n=2) or tumor bearing mice treated with vehicle (n=4) or tofacitinib (n=4) were digested and assayed by flow cytometry for the presence of $CD11b^+$ cells. Mixed splenocyte populations were stained with anti-CD45 and anti-CD11b. Cell counts for $CD45^+/CD11b^+$ cells are shown, normalized to 100,000 total splenocytes for each mouse. B. Spleens were harvested as above. Mixed splenocyte populations were stained with anti-CD45 and anti-CD68. Cell counts for $CD45^+/CD68^+$ cells are shown, normalized to 100,000 total splenocytes for each mouse.